Original Article

DOI: http://dx.doi.org/10.16926/par.2018.06.06

Analysis of two methods indicating the shoulder joint angles using three dimensional data

Maria Skublewska-Paszkowska[ABD], Michal Dekundy[AD], Edyta Lukasik[BD], Jakub Smolka[B]

Institute of Computer Science, Lublin University of Technology

Authors' Contribution: A – Study Design, B – Data Collection, C – Statistical Analysis, D – Manuscript Preparation, E – Funds Collection

Abstract

The article contains a comparative analysis of two methods of calculating angles in the shoulder joint of the right upper limb. For the purposes of this study, a marker-vector method was developed that calculates angles based on retroreflective 3D marker's positions and vectors created on the basis of their positions. Movements from two types of sports (sword fighting and tennis forehand) were analysed. These movements were recorded using an optical motion capture system. The obtained results were compared with the values read from the Plug-in Gait biomechanical model from C3D files. The results show that the proposed method is more universal and can be used independently. In addition, the Plug-in Gait model is not adequate for the analysis of the acquired shoulder angles of tennis players.

Keywords: motion capture, C3D file, angle calculation methods, Plug-in Gait biomechanical model

Address for correspondence: Maria Skublewska-Paszkowska, Institute of Computer Science, Lublin University of Technology, Poland; email: maria.paszkowska@pollub.pl

Recevied: 20.11.2017; Accepted: 15.01.2018; Published online: 7.03.2018

Cite this article as: Skublewska-Paszkowska M, Dekundy M, Lukasik E, Smolka J. Analysis of two methods indicating the shoulder joint angles using three dimensional data. Physical Activity Review 2018; 6: 37-44. doi: 10.16926/par.2018.06.06

INTRODUCTION

The movement analyses using inertial and optical motion capture technologies have been widely developed in many scientific fields, because they provide values of specified body and joints positions. Many of optical motion capture systems concern the implemented biomechanical models which calculate additional values such as angles, forces or moments between the human joints. The calculations are made on the basis of the markers' placement on the participant's body and the additional values input to the system (e.g. weight, height and the length of the specified limbs). The inertial systems provide the angles based on the attached IMU sensors [1].

Optical motion capture systems are precise and are thus involved in athlete analyses [2]. They concern the parameters available after recording motion capture sessions, such as velocities, accelerations, stroke execution times [3,4,5], as well as ranges of motion or speeds of joints [6]. The Vicon Plug-in Gait (PiG) model allows the researchers to extend their studies of many important calculations, very often necessary for motion analyses in many sport fields [6,7]. The analysis of the professional tennis players using this biomechanical model is presented in [8] while training on an indoor ergometer in [9].

The PiG biomechanical model is widely used for examinations involving human participations, because it is a conventional gait analysis model. It is not always efficient as a research tool and thus it is sometimes necessary to extend it by implementing additional functionality [10]. There are also studies of new models and their comparison to the Plug-in-Gait model. The studies cover comparing joint kinematics obtained by this model with those produced by a widely used Inverse Kinematics model available with the OpenSim distibution [11]. A new Two-marker-model, which calculates the joint centre, was tested [12]. It can be considered alternatively to the PiG model because the error analysis showed a smaller error than with PiG. Foot movements using the Vicon system have been studied in man's gait [13,14]. The PiG model used in gait analysis is not adequate because it considers the foot as a rigid segment [15]. The multi-segment Wang-foot model to measure the foot and the ankle kinetic and kinematic data during gait was developed and validated [16].

Due to the fact that the angles obtained by the model are not always correct, the idea of this paper is to compare the shoulder angles received by the PiG model with the author's method based on the retroreflective markers attached to the participant's body called marker-vector method (M-V). The markers were attached according to Plug-in Gait specification [17] so that the analysis could be more precise. The tennis forehand and sword techniques were analysed. The following thesis is formulated in the paper "The presented marker-vector method is suitable for calculating angles in sport disciplines". The thesis is proved by the obtained results.

MATERIAL AND METHODS

Participants

Two men participated in the study. The first (age 26, height 1.84 m, weight 120 kg) performed sword fighting and the second (age 30, height 1.74 m, weight 71 kg) tennis forehand strokes without the ball. They signed the ethical approval form for this research.

The participants were prepared for the experiment according to the Plug-in Gait Model [17]. Thirty-nine retroreflective markers were attached to the participants using hypo-allergenic double-sided tape as specified in the model. This model allows for calculating angles, torques and forces in a subject's joints. Then, the persons were measured for the purpose of creating and scaling the new subjects in the Nexus software (height, weight, leg length, arm offset, knee, ankle, elbow and the thickness of both hands). The calibrations of the subjects were performed as the next step in preparation due to the verification that the markers are visible and correctly attached.

After a 15-minute warm-up, the first participant made a series of moves with a sword called a waltz. The participant moved forward by performing two alternating swings with two-handed swords. He then performed the same rotation by moving backwards and returning to the starting position. The second participant was told to perform eleven forehand strokes without the ball while running and

avoiding a bollard placed on the floor. Because the participant was running, the strokes were more natural than hitting the ball from a standing pose.

Data acquisition

A passive optical motion capture system was used to track the participants while performing exercises at the Laboratory of Motion Analysis and Interface Ergonomics at the Lublin University of Technology in Poland where interdisciplinary tests are performed [18]. The motion capture system consisted of: eight NIR T40S cameras operating in near infrared, two reference video Bonita cameras, a Giganet hub collecting data, a desktop computer and a set of accessories (e.g. markers, a calibration wand, double-sided tape). The system recorded the positions of the markers placed on the subject's body (each marker must be seen by at least two cameras). The equipment was supplied with Vicon's Nexus 2.0 software, used for system calibration, data recording and data processing. The movements were registered with 100 Hz.

Each capture session created a set of files. During capture an additional video file containing examined person data and additional information was created. This file, for security purposes, may be watermarked with robust algorithm [19].

Marker-vector method

The presented method for calculating angles for the participant's shoulder is based on the three dimensional coordinates stored in C3D files. The marker's names and locations are exactly the same with the PiG model specification. The described method does not include the approximation of bone positions in the upper limb. However, the method is not limited to the specified angles. It may be used to compute any angle of the participant's body, even not involved with the skeleton.

Three local coordinate systems were created to calculate the positions of the markers used for determining the three right hand shoulder angles. The local chest coordinate system was created as follows: first, the direction of the Y axis was calculated as the T10-STRN vector. Then the origin of the system was defined – a point on the Y axis line forming a vector perpendicular to the Y axis and passing through C7. Axis Z was designated as the direction of the origin – C7. The X axis was denoted as a cross product of Y axis and Z axis vectors.

The local coordinate system of the shoulder bone was created as follows: first the Z axis was created as the direction vector RSHO (Right Shoulder) – RELB (Right Elbow). The origin of the coordinate system was defined as a point on the Z axis forming a vector from the RUPA (Right Upper Arm) perpendicular to the Z axis. The X axis was assumed to be the origin – RUPA vector. The Y axis was calculated as the cross product of X and Z axis vectors.

The origin of the radial bone coordinate system was the midpoint between the RWRA (Right wrist bar thumb side) and RWRB (Right Wrist bar pinkie side) markers. The X axis was the direction from the origin to the RELB marker and the Y axis from RWRB to RWRA. The Z axis was the cross product of the remaining axes.

The next step was to convert the points from the global to the local coordinate system. Transformation of a point into a local coordinate system is given by the following formula (1) [19],

$$\begin{aligned} x' &= (P_1 - P_2) \cdot u_x \\ y' &= (P_1 - P_2) \cdot u_y \\ z' &= (P_1 - P_2) \cdot u_z \end{aligned} \qquad (1)$$

where: P_1 – the point with global coordinates, P_2 – the origin of local coordinate system, u_x, u_y, u_z – mutually orthogonal unit vectors representing local coordinate system, x', y', z' – new local coordinates of point P_1. The symbol · is the dot product.

The rotation of point P (x_p, y_p, z_p) by the angle α around the axes X, Y, Z of the coordinate system passing through the point (x_c, y_c, z_c), needed to undo the previous rotation in the sequence of moves possible in a given joint, is described by formulae (2), (3), (4) [20].

$$\begin{aligned} x' &= x_p \\ y' &= (y_p - y_c) \cdot cos(\alpha) - (z_p - z_c) \cdot sin(\alpha) + y_c \\ z' &= (y_p - y_c) \cdot sin(\alpha) + (z_p - z_c) \cdot cos(\alpha) + z_c \end{aligned} \quad (2)$$

$$\begin{aligned} x' &= (x_p - x_c) \cdot cos(\alpha) - (z_p - z_c) \cdot sin(\alpha) + x_c \\ y' &= y_p \\ z' &= (x_p - x_c) \cdot sin(\alpha) + (z_p - z_c) \cdot cos(\alpha) + z_c \end{aligned} \quad (3)$$

$$\begin{aligned} x' &= (x_p - x_c) \cdot cos(\alpha) - (y_p - y_c) \cdot \sin(\alpha) + x_c \\ y' &= (x_p - x_c) \cdot sin(\alpha) - (y_p - y_c) \cdot \cos(\alpha) + y_c \\ z' &= z_p \end{aligned} \quad (4)$$

As with the Plug-in Gait model, Euler angles are the end result. Listing 1 shows the method of calculating the Euler angles – the atan2 function of which the first parameter is a determinant proportional to the sine, and the second – a dot product proportional to the cosine of the angle between vectors v1 and v2, giving the angle [20].

Listing 1. Calculating the Euler angles between vectors v1 and v2.

```
float detx = v1.y*v2.z – v1.z*v2.y;
float dotx = v1.y*v2.y + v1.z*v2.z;
float angleX = atan2(detx, dotx);

float dety = v1.x*v2.z – v1.z*v2.x;
float doty = v1.x*v2.x + v1.z*v2.z;
float angleY = atan2(dety, doty);

float detz= v1.x*v2.y – v1.y*v2.x;
float dotz= v1.x*v2.x + v1.y*v2.y;
float angleZ = atan2(detz, dotz);
```

Depending on the axis of rotation, two components of vectors v1 and v2 are considered. The result is the angles in the interval [-π, π].

Plug-in Gait model

The model defines a number of angles associated with the deflection of the major joints representing the human skeleton. In this article, the angle of the right upper limb (RShoulderAngles) was analysed. Each of the angles contains three components counted as rotation around the individual axes of the coordinate system (Euler angles) associated with the local skeleton segment.

The shoulder joints defined in the Plug-in Gait model are:

- Flexion/Extension – between the negative axis Z of the thorax and the RSHO-RELB vector around the Y axis of the thorax,
- Abduction – between the negative axis Z of the thorax and the RSHO-RELB vector around the X' axis of the thoracic system, rotated by the previous rotation,
- Internal Rotation – between the Y axis of the chest and the RELB-RWRA vector around the Z axis of the chest, rotated by two previous rotations.

The results obtained from the PiG model were read from C3D files using the piece of software created for the purpose of the analysis. Due to the fact that the model uses Cardan (Euler) in order to calculate joint angles, Gimbal Lock and Codman's Paradox [20] may occur in particular shoulder positions. Although the described model includes some steps that make an effort to minimise the

above effects by trying to keep the shoulder angles in consistent and understandable quadrants, this problem may appear [17].

The results obtained from the PiG model were read from C3D files using the piece of software created for the purpose of the analysis. Due to the fact that the model uses Cardan (Euler) in order to calculate joint angles, Gimbal Lock and Codman's Paradox [21] may occur in particular shoulder's poses. Although, the described model includes some steps that make an effort to minimize the above effects by trying to keep the shoulder angles in consistent and understandable quadrants, this problem may appear [17].

RESULTS

The obtained results of the angles of the right shoulder joint are shown in Figures 1-6. The data from the proposed M-V method were marked in red, and in green – the graph of the data read from the PiG model. Three movements have been analysed: flexion, abduction and internal rotation. For each of the presented results the following measures were computed: (1) the mean of all differences (between values from PiG and M-V), (2) the maximum difference and (3) the minimum difference (Tables: 1, 2 and 3). The analysis concerns two types of motion. First, the waltz sword movement, and second – eleven forehand strokes.

Shoulder flexion

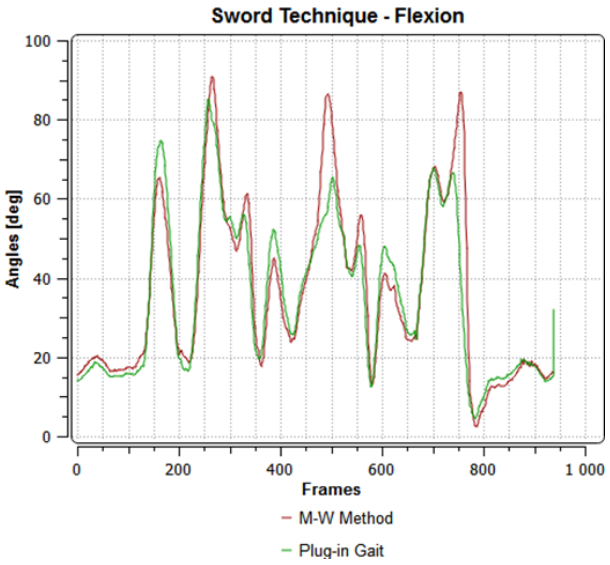

Figure 1. Flexion angle of the shoulder joint for the sword swing

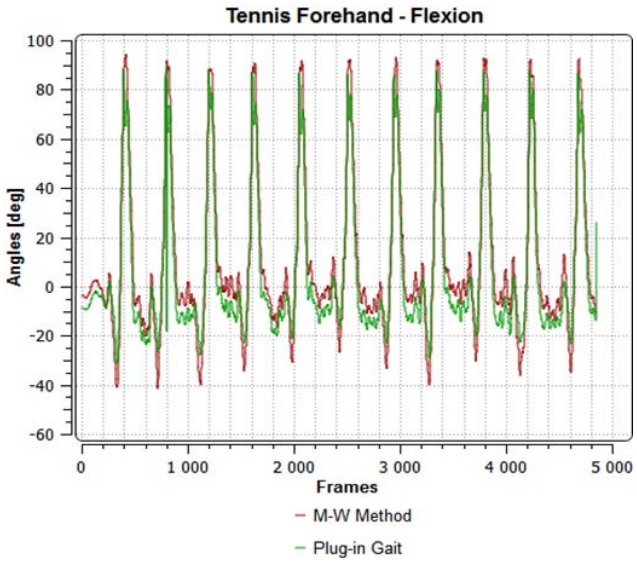

Figure 2. Flexion angle of the shoulder joint for the forehand stroke

Tab. 1. Angles differences in shoulder joint flexion

Type of movement	Mean difference [°]	Maximum difference [°]	Minimum difference [°]
Sword	4.75	52.19	0.01
Tennis Forehand	7.40	107.29	0.01

Shoulder abduction

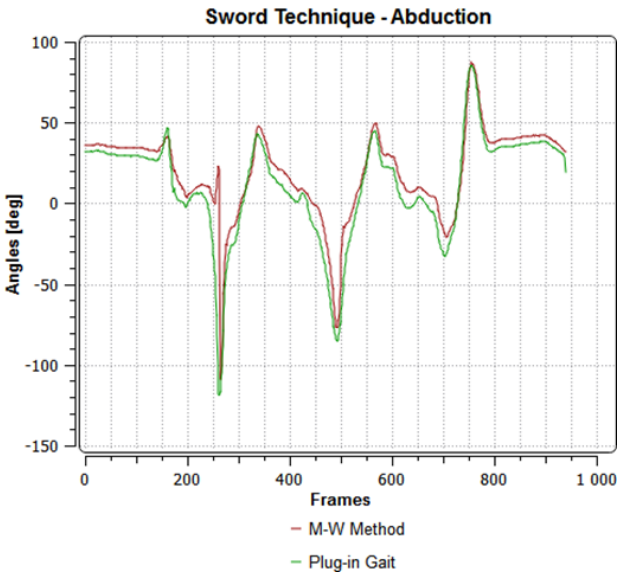

Figure 3. Abduction angle for the shoulder joint for the sword swing

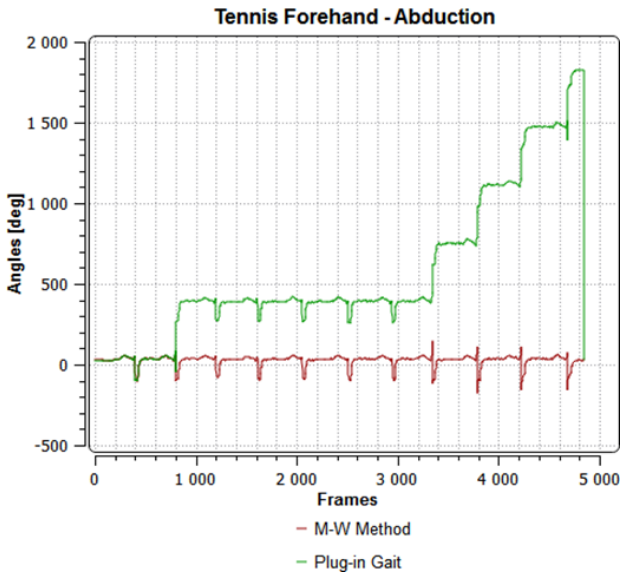

Figure 4. Abduction angle for the shoulder joint for the forehand stroke

Tab. 2. Angle differences for abduction in the shoulder

Type of movement	Mean difference [°]	Maximum difference [°]	Minimum difference [°]
Sword	8.60	141.71	0.04
Tennis Forehand	547.79	1851.01	0.00

Angles returned by the PiG model for the forehand stroke go significantly beyond the range corresponding to the human motion angle.

Shoulder internal rotation

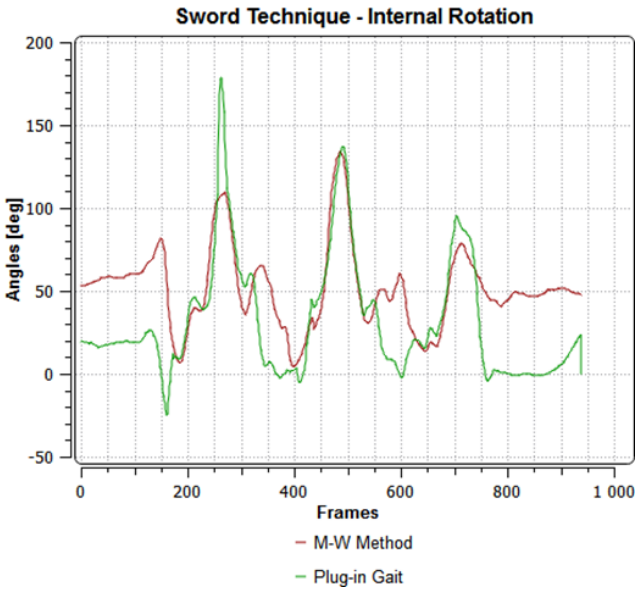

Figure 5. internal rotation angle for the shoulder joint for the sword swing

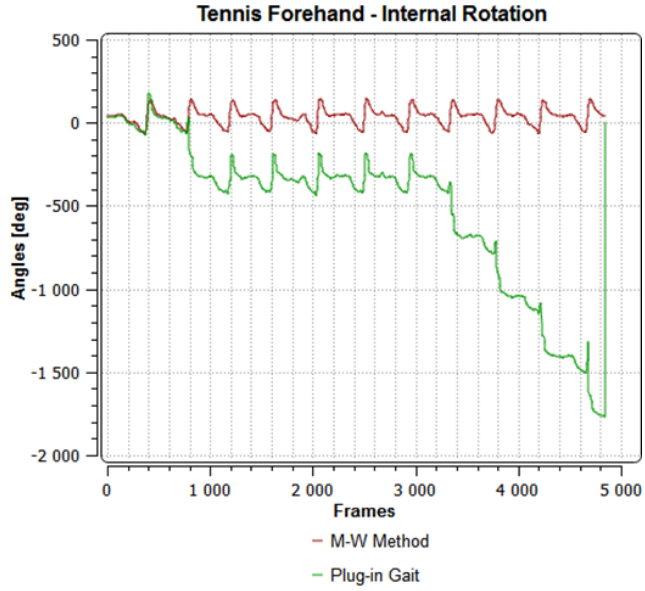

Figure 6. Internal rotation angle for the shoulder joint for tennis forehand stroke

Tab. 3. Angles differences for internal rotation in the shoulder joint

Type of movement	Mean difference [°]	Maximum difference [°]	Minimum difference [°]
Sword	27.16	91.38	0,03
Tennis Forehand	561.72	1842.89	0.32

As in the case of abduction, the results from the PiG model return values beyond the possible angles of a forehand stroke.

CONCLUSIONS

The shoulder joint angles were examined in two types of movements: sword fighting and tennis forehand stroke. Two models generating angular values were compared: the PiG model (by Vicon Ltd) and the proposed M-V method. Each angle is defined by three coordinates (Euler angles) in three-dimensional space. The flexion values in both types of movement (Fig. 1-2) show relatively small average differences between the two models. They are 4.75° for sword fighting and 7.40° for forehand stroke (Table 1). The Shoulder abduction value (Fig. 3-4) generates a mean difference of 11.86° in sword motion and 547.79° in forehand stroke (Table 2). Similar results were obtained for internal rotation (Fig. 5-6) in the shoulder joint: 27.16° in sword fighting and 550.24° in forehand stroke (Table 3). The angle values generated in the PiG model during the forehand stroke significantly exceeded the correct angle values that should lie within the $[0, 2\pi]$ interval.

The marker-vector method is characterised by greater versatility, due to which it is also possible to calculate angles between markers outside the Plug-in Gait definition. In addition to the results provided by the Plug-in Gait model, the results of the abduction and internal rotation produced by the marker-vector method for tennis are correct. They are not disadvantaged by the Gimbal Lock or Codman's paradox phenomena. It should be remembered that the marker-vector method does not take into account the position of the bones of the human skeleton.

ACKNOWLEDGEMENTS

The research programme "Biomechanical parameters of athletes in individual exercises", based on the analysis of 3D motion data and EMG, realised in the Laboratory of Motion Analysis and Interface Ergonomics of the Lublin University of Technology, was approved by the Commission for Research Ethics, No. 2/2016 dated 8.04.2016. The authors would like to thank the student club Tennis Academy POL-SART and the Lublin University of Technology students for their support.

REFERENCES

1. Kopniak P, Kaminski M. Natural interface for robotic arm controlling based on inertial motion capture. 9th International Conference on Human System Interactions, New York. IEEE 2016: 110-116.
2. Pueo B, Jimenez-Olmedo J. M. Application of motion capture technology for sport performance analysis. Federación Española de Asociaciones de Docentes de Educación Física (FEADEF) 2016: 241-247.
3. Wasik J. Kinematics and Kinetics of Taekwon-do Side Kick. Journal of Human Kinetics 2011; 30: 13-20. doi: 10.2478/v10078-011-0068.
4. Wasik J, Shan GB. Factors influencing the effectiveness of axe kick in taekwon-do. Archives of Budo 2014; 10: 29-36.
5. Ortenburger D, Wąsik J, Góra T. Selected dimensions of the self-esteem and a kinematic effect of the intentional target at taekwondo athletes. Arch Budo Sci Martial Art Extreme Sport 2016; 12: 117-121.
6. Yu DF, Yu YG, Wilde B, et al. Biomechanical characteristics of the Axe Kick in Tae Kwon-Do. Archives of Budo, 8(4): 213-218.
7. Preuschl E., Hassmann M., Baca A. A Kinematic Analysis of the Jumping Front-Leg Axe-Kick in Taekwondo. Journal of Sports Science And Medicine 2016; 15(1): 92-101.
8. Skublewska-Paszkowska M. Motion Repeatability of Tennis Forehand Preparation Phase Without the Ball Using Three Dimensional Data. Proceedings of 38th International Conference on Information Systems

Architecture and Technology (ISAT 2017); 17-19 September 2017; Szklarska Poręba, POLAND. Advances in Intelligent Systems and Computing 656: 156-165. doi: 10.1007/978-3-319-67229-8_14.
9. Skublewska-Paszkowska M., Lukasik E., Montusiewicz J. Analysis of rowing based on handle trajectory. Procedings of the 9th International Conference on Human System Interactions (HSI); 6-8 July 2016; Portsmouth, UK. Conference on Human System Interaction: 62-68.
10. Stambolian D., Asfour S., Eltoukhy M. Using Vicon Bodybuilder and Plug-In-Gait to Generate L5/S1 Angles, Forces and Moments; 1-4 march 2014; Big Sky, MT. 2014 IEEE Aerospace Conference: 1-7.
11. Kainz H, Modenese L, Lloyd DG, et al. Joint kinematic calculation based on clinical direct kinematic versus inverse kinematic gait model. Journal of Biomechanics 2016; 49: 1658-1669.
12. Nair SP, Gibbs S, Arnold G, et al. A method to cjnalculate the centre of the ankle joint: A comparison with the Vicon Plug-in-Gait model. Clinical Biomechanics 2010; 25: 582-587.
13. Daniilidis K, Jakubowitz E, Thomann A, et al. Does a foot-drop implent improve kinetic and kinematic parameters in the foot and ankle. Arch Orthop Trauma Surg 2017; 137: 499-506;
14. Krumm D, Cockcroft J, Zaumseil F, Odenwald S. Analytical evaluation of the effects of inconsistent anthropometric measurements on joint kinematics in motion capturing. Gait & Posture 2016; 46: 1-4.
15. Rigney SM, Simmons A, Kark L. A prosthesis-specific multi-link segment model of lower-limb amputee sprinting, Journal of Biomechanics 2016; 49: 3185-3193.
16. Yalamanchili SB, Surapaneni SB, Wang W, et al. The evaluation of foot joint angles and forces during walking, J. Evolution Med. Dent. Sci. 2017; 6(2): 124-131.
17. VICON, 2016. Plug-in Gait Product Guide [WWW Document]. VICON. URL https://www.vicon.com/downloads/documentation/plug-in-gait-product-guide (accessed 20.10.2017).
18. Skublewska-Paszkowska M, Lukasik E, Smolka J. et al. Comprehensive measurements of human motion parameters in research projects. Procedings of the 10th International Technology, Education and Development Conference INTED, 6-9 March 2016, Valencia, Spain: IATED Academy 2016: 8597-8605.
19. Koziel G. Simplified Steganographic Algorithm Based on Fourier Transform. Advanced Science Letters 2014; 20(2): 505-509. doi: 10.1166/as1.2014.5322.
20. Bajd T, Mihelj M, Munih M. Introduction to Robotics. Springer 2013.
21. Klimkiewicz J. Wiliams G, Sher J. et. al. The acromioclavicular capsule as a restraint to posterior translation of the clavicle: A biomechanical analysis. J. Shoulder Elbow Surg 1991; 8: 181-192.